

Supporting information

Effect of porphyrin loading on performance of dye sensitized solar cells based on iodide/tri-iodide and cobalt electrolytes

Ana Aljarilla,^a John N. Clifford,*^b Laia Pellejà,^b Antonio Moncho,^b Susana Arrechea,^a Pilar de la Cruz,^a Fernando Langa*^a and Emilio Palomares*^{b,c}

^a Instituto de Nanociencia, Nanotecnología y Materiales Moleculares (INAMOL), Universidad de Castilla-La Mancha, 45071-Toledo, Spain

^b Institute of Chemical Research of Catalonia (ICIQ), Avda. Països Catalans 16, Tarragona E-43007, Spain

^c ICREA, Avda. Lluís Companys 28, Barcelona E-08030, Spain

E-mail: Fernando.Langa@uclm.es, jnclifford@iciq.es

Table of contents

1- Experimental conditions	S1
2- ^1H NMR, ^{13}C NMR, FT-IR and MALDI-TOF	S2
3- UV-Visible and emission spectroscopies	S14
4- Cyclic and Square Wave Voltammetry plots of 1a and 1b	S16
5- Thermogravimetric analysis of 1a and 1b	S18

1.- Experimental conditions

Synthetic procedures were carried out under inert argon atmosphere, in dry solvent unless otherwise noted. All reagents and solvents were reagent grade and were used without further purification. Chromatographic purifications were performed using silica gel 60 SDS (particle size 0.040-0.063 mm). Analytical thin-layer chromatography was performed using Merck TLC silica gel 60 F254. ¹H NMR spectra were obtained on Bruker TopSpin AV-400 (400 MHz) spectrometer. Chemical shifts are reported in parts per million (ppm) relative to the solvent residual peak (CDCl₃, 7.27 ppm). ¹³C NMR chemical shifts are reported relative to the solvent residual peak (CDCl₃, 77.00 ppm). UV-Vis measurements were carried out on a Shimadzu UV 3600 spectrophotometer. For extinction coefficient determination, solutions of different concentration were prepared in CH₂Cl₂, HPLC grade, with absorption between 0.1-1 of absorbance using a 1 cm UV cuvette. The emission measurements were carried out on Cary Eclipse fluorescence spectrophotometer. Mass spectra (MALDI-TOF) were recorded on a VOYAGER DE™ STR mass spectrometer using dithranol as matrix. Melting points are uncorrected.

The molecular geometries and frontier molecular orbitals of these new dyes have been optimized by density functional theory (DFT) calculations at the B3LYP/6-31G* level.¹

Cyclic voltammetry was performed in THF (4:1) solutions. Tetrabutylammonium perchlorate (0.1 M as supporting electrolyte) were purchased from Acros and used without purification. Solutions were deoxygenated by argon bubbling prior to each experiment which was run under argon atmosphere. Experiments were done in a one-compartment cell equipped with a platinum working microelectrode ($\varnothing = 2$ mm) and a platinum wire counter electrode. An Ag/AgCl electrode was used as reference and checked against the ferrocene/ferrocenium couple (Fc/Fc⁺) before and after each experiment.

¹ Gaussian 03, Revision D.02, Frisch, M. J.; Trucks, G. W.; Schlegel, H. B.; Scuseria, G. E.; Robb, M. A.; Cheeseman, J. R.; Montgomery Jr., J. A.; Vreven, T.; Kudin, K. N.; Burant, J. C.; Millam, J. M.; Iyengar, S. S.; Tomasi, J.; Barone, V.; Mennucci, B.; Cossi, M.; Scalmani, G.; Rega, N.; Petersson, G. A.; Nakatsuji, H.; Hada, M.; Ehara, M.; Toyota, K.; Fukuda, R.; Hasegawa, J.; Ishida, M.; Nakajima, T.; Honda, Y.; Kitao, O.; Nakai, H.; Klene, M.; Li, X.; Knox, J. E.; Hratchian, H. P.; Cross, J. B.; Bakken, V.; Adamo, C.; Jaramillo, J.; Gomperts, R.; Stratmann, R. E.; Yazyev, O.; Austin, A. J.; Cammi, R.; Pomelli, C.; Ochterski, J. W.; Ayala, P. Y.; Morokuma, K.; Voth, G. A.; Salvador, P.; Dannenberg, J. J.; Zakrzewski, V. G.; Dapprich, S.; Daniels, A. D.; Strain, M. C.; Farkas, O.; Malick, D. K.; Rabuck, A. D.; Raghavachari, K.; Foresman, J. B.; Ortiz, J. V.; Cui, Q.; Baboul, A. G.; Clifford, S.; Cioslowski, J.; Stefanov, B. B.; Liu, G.; Liashenko, A.; Piskorz, P.; Komaromi, I.; Martin, R. L.; Fox, D. J.; Keith, T.; Al-Laham, M. A.; Peng, C. Y.; Nanayakkara, A.; Challacombe, M.; Gill, P. M. W.; Johnson, B.; Chen, W.; Wong, M. W.; Gonzalez, C.; Pople, J. A. Gaussian, Inc., Wallingford CT, 2004.

2.- ^1H NMR, ^{13}C NMR, FT-IR and MALDI-TOF

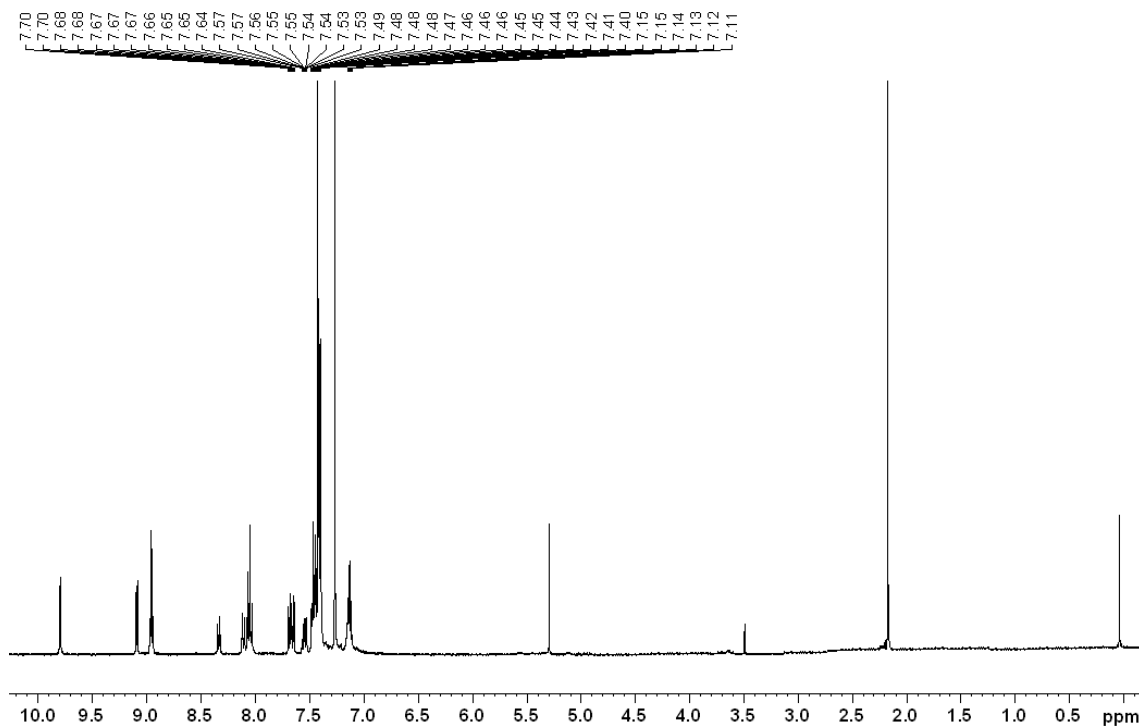


Figure S1. ^1H NMR spectrum (400 MHz, CDCl_3) of compound **1a**.

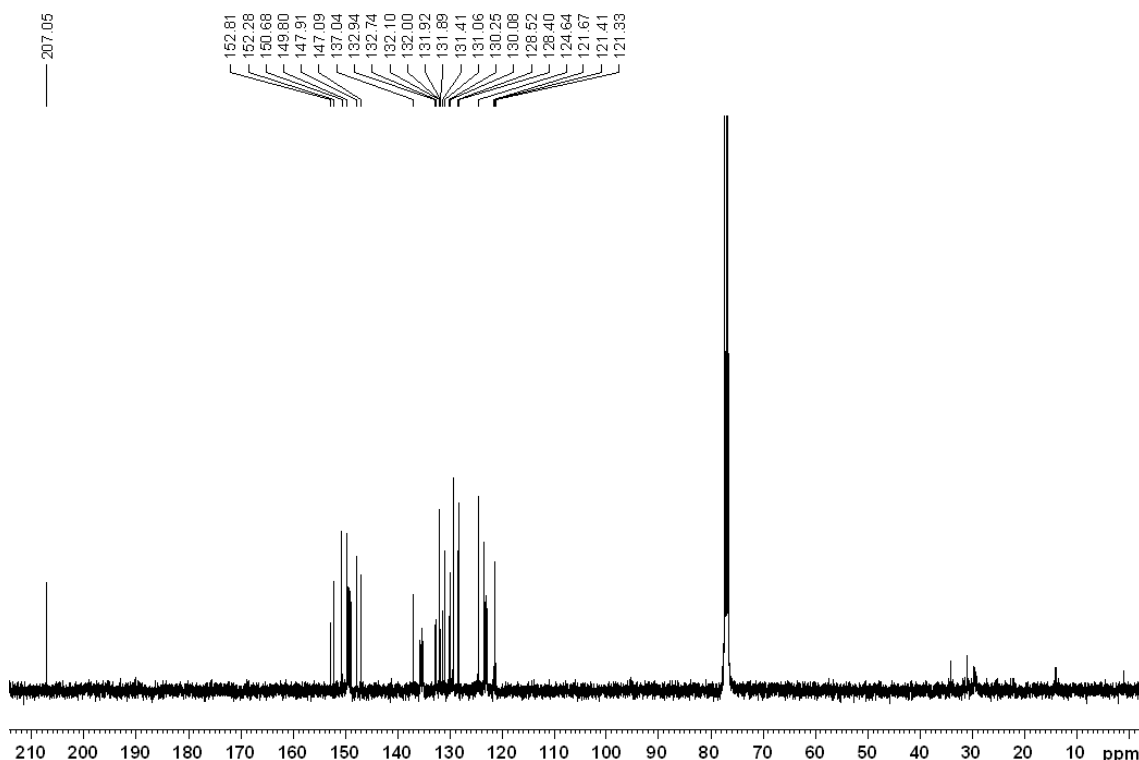


Figure S2. ^{13}C NMR spectrum (100 MHz, CDCl_3) of compound **1a**.

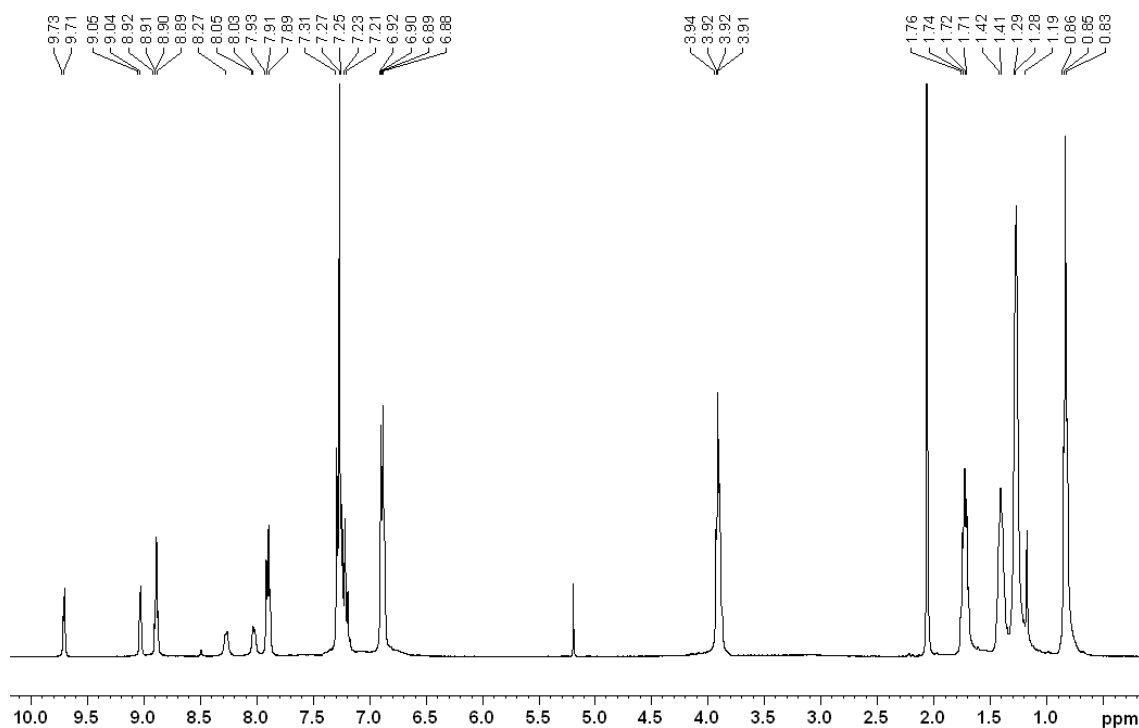


Figure S3. ¹H NMR spectrum (400 MHz, CDCl₃) of compound **1b**.

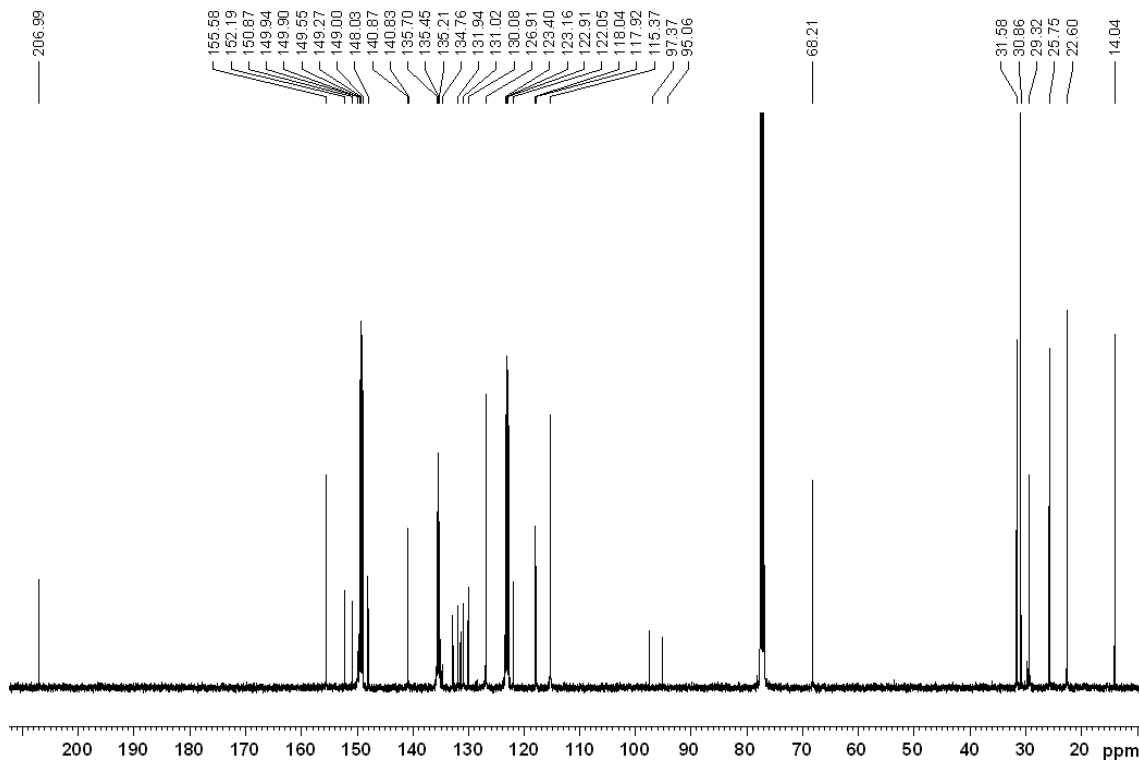


Figure S4. ¹³C NMR spectrum (100 MHz, CDCl₃) of compound **1b**.

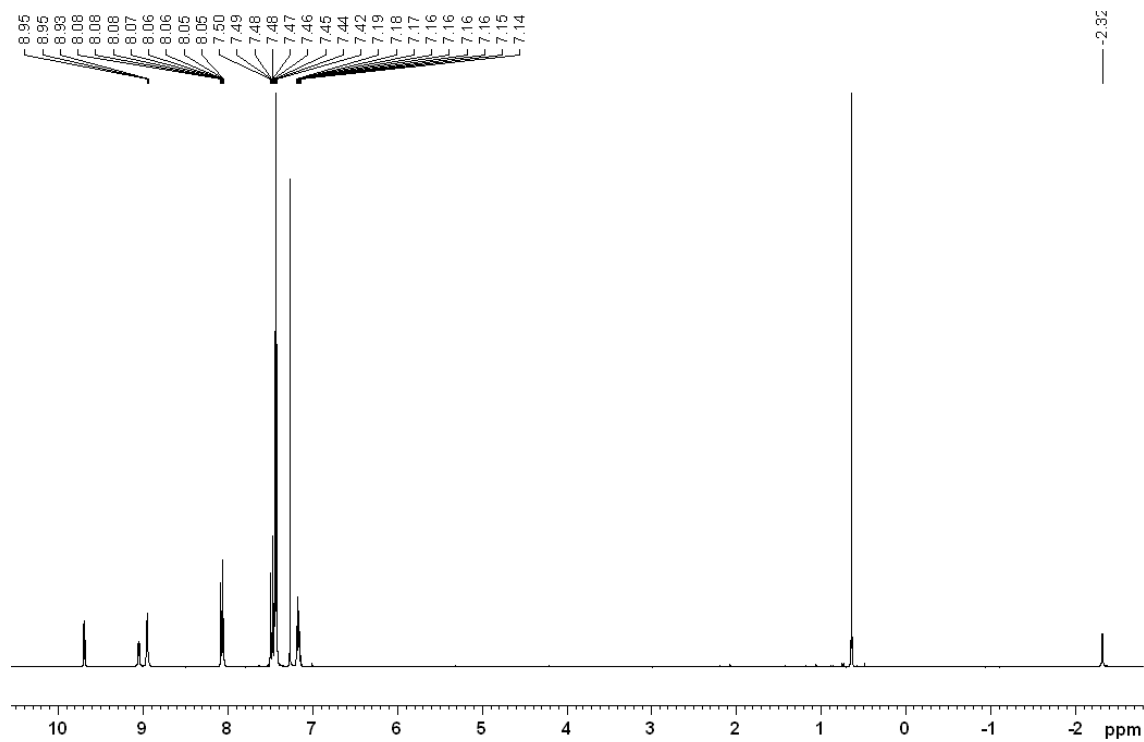


Figure S5. ¹H NMR spectrum (400 MHz, CDCl₃) of compound 2a.

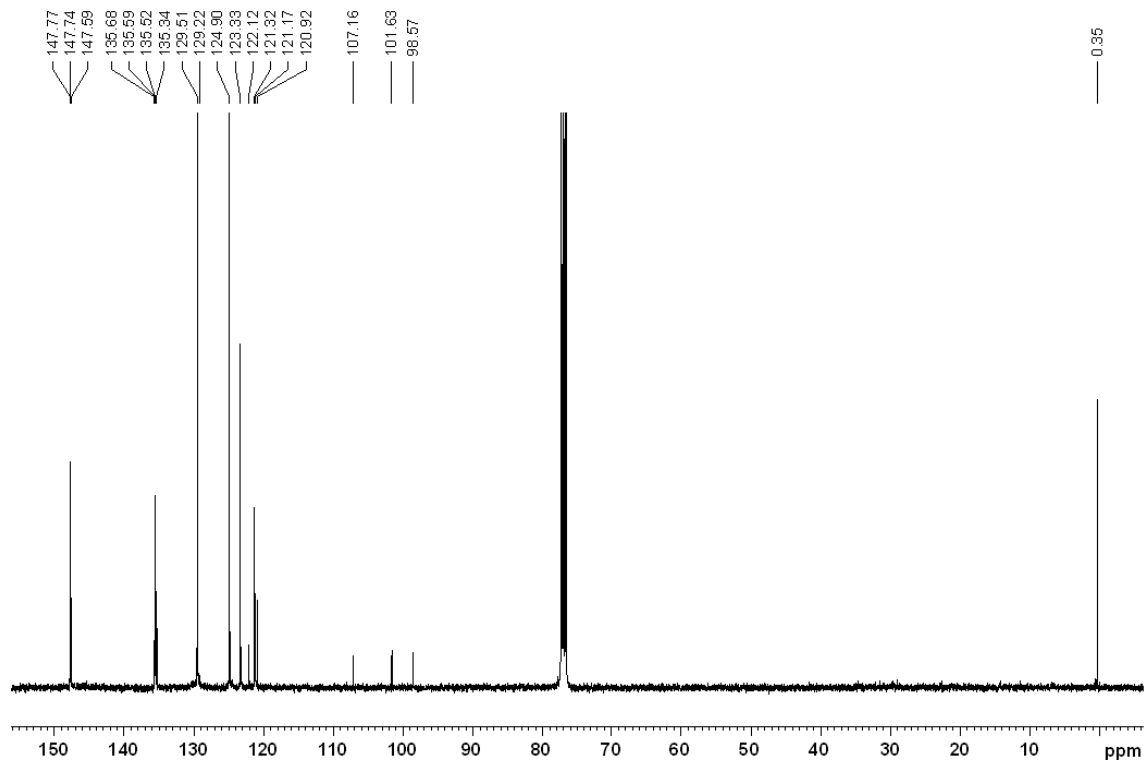


Figure S6. ¹³C NMR spectrum (100 MHz, CDCl₃) of compound 2a.

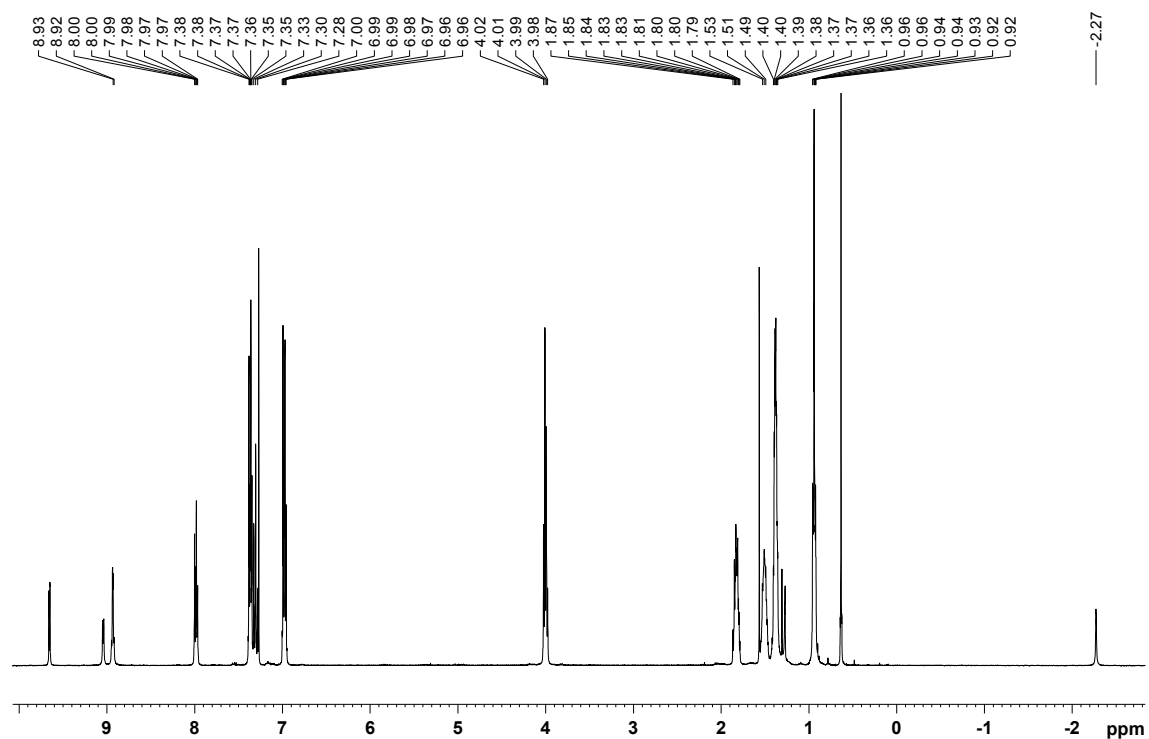


Figure S7. ^1H NMR spectrum (400 MHz, CDCl_3) of compound **2b**.

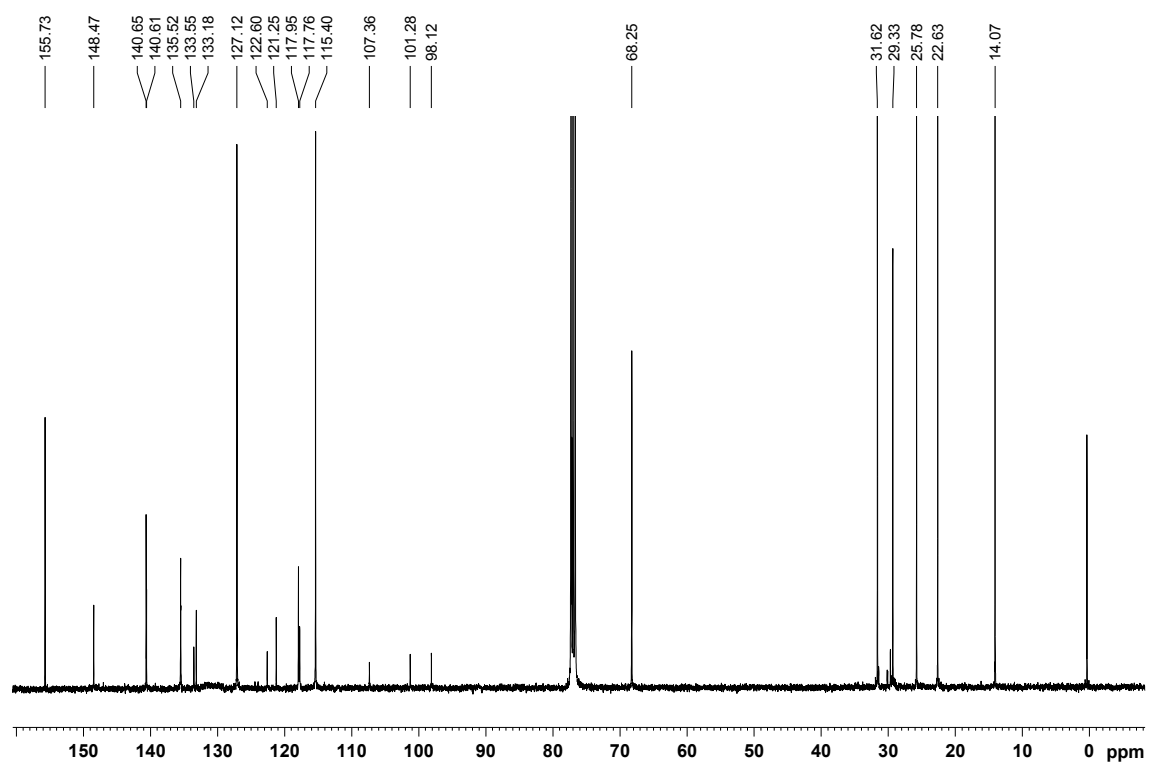


Figure S8. ^{13}C NMR spectrum (100 MHz, CDCl_3) of compound **2b**.

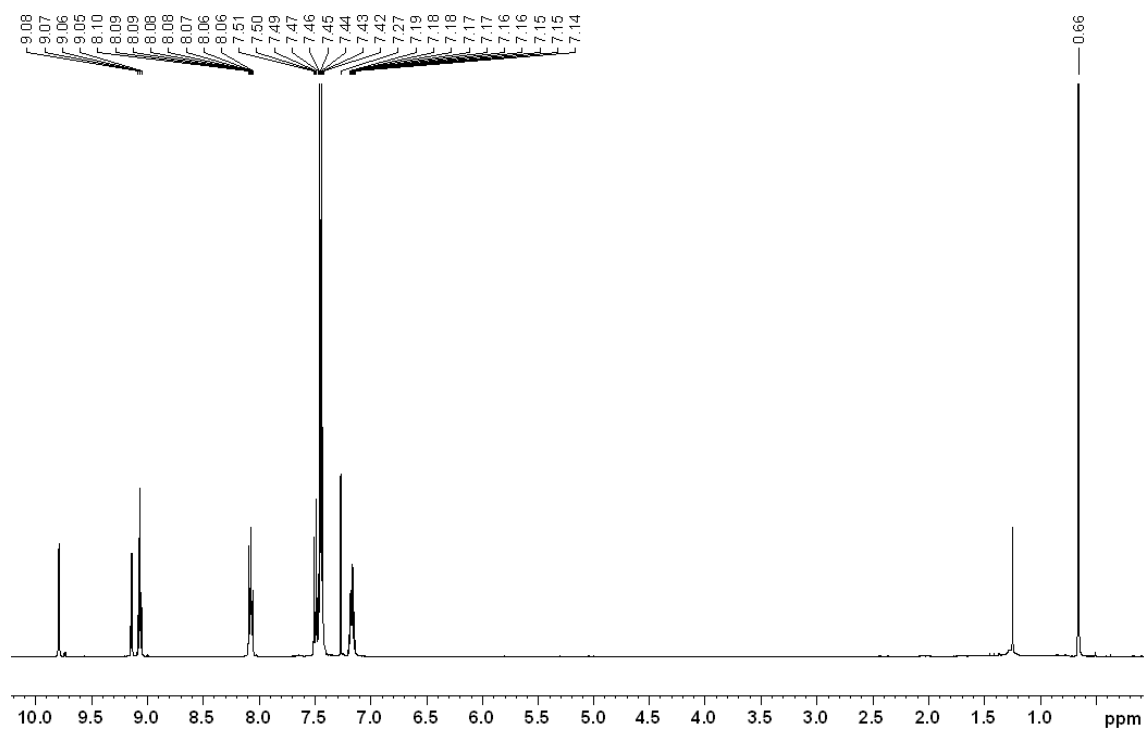


Figure S9. ¹H NMR spectrum (400 MHz, CDCl₃) of compound 3a.

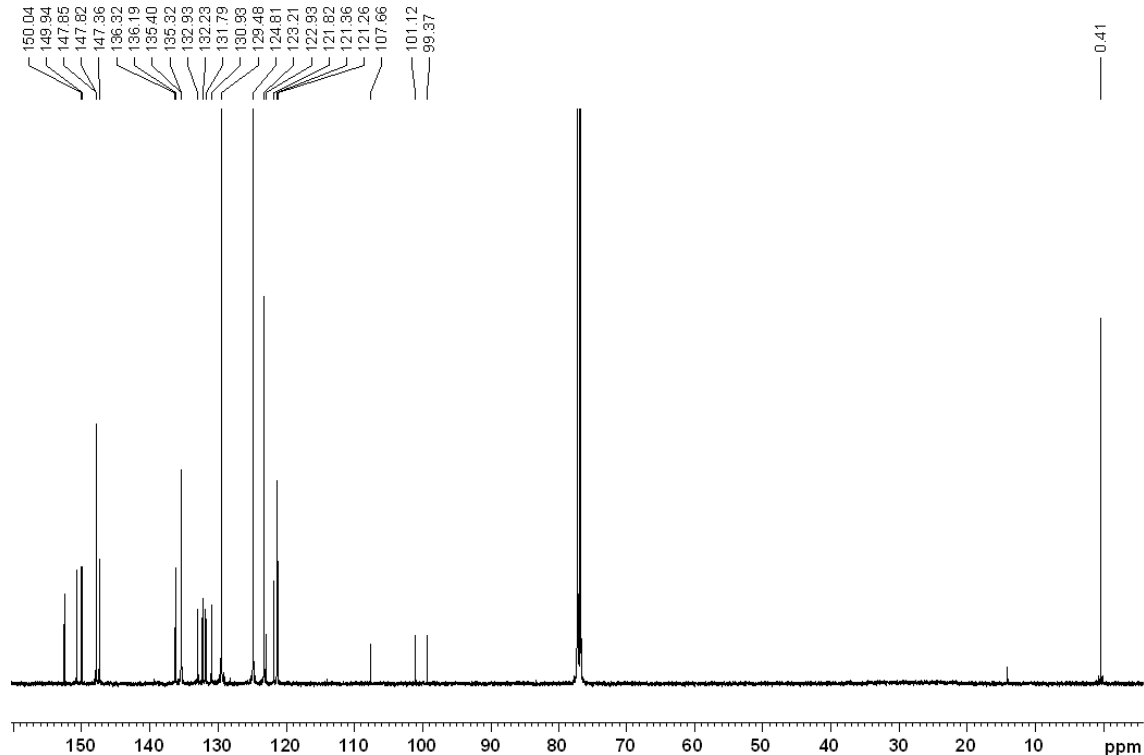


Figure S10. ¹³C NMR spectrum (100 MHz, CDCl₃) of compound 3a.

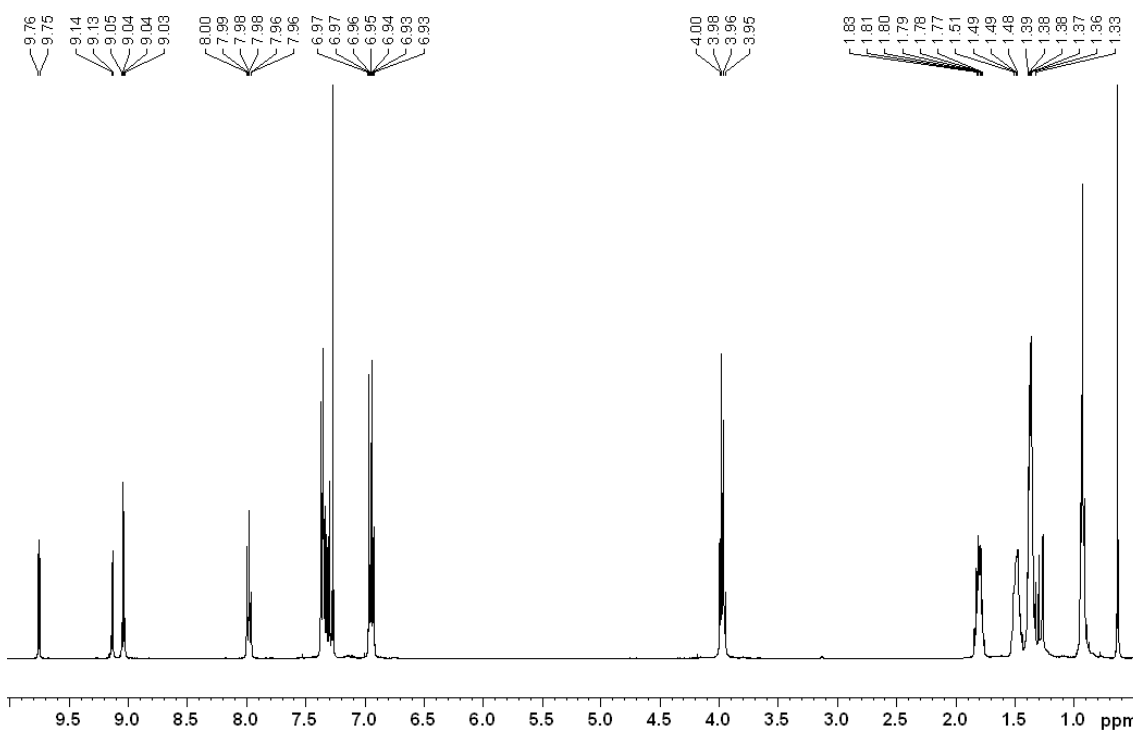


Figure S11. ¹H NMR spectrum (400 MHz, CDCl₃) of compound 3b.

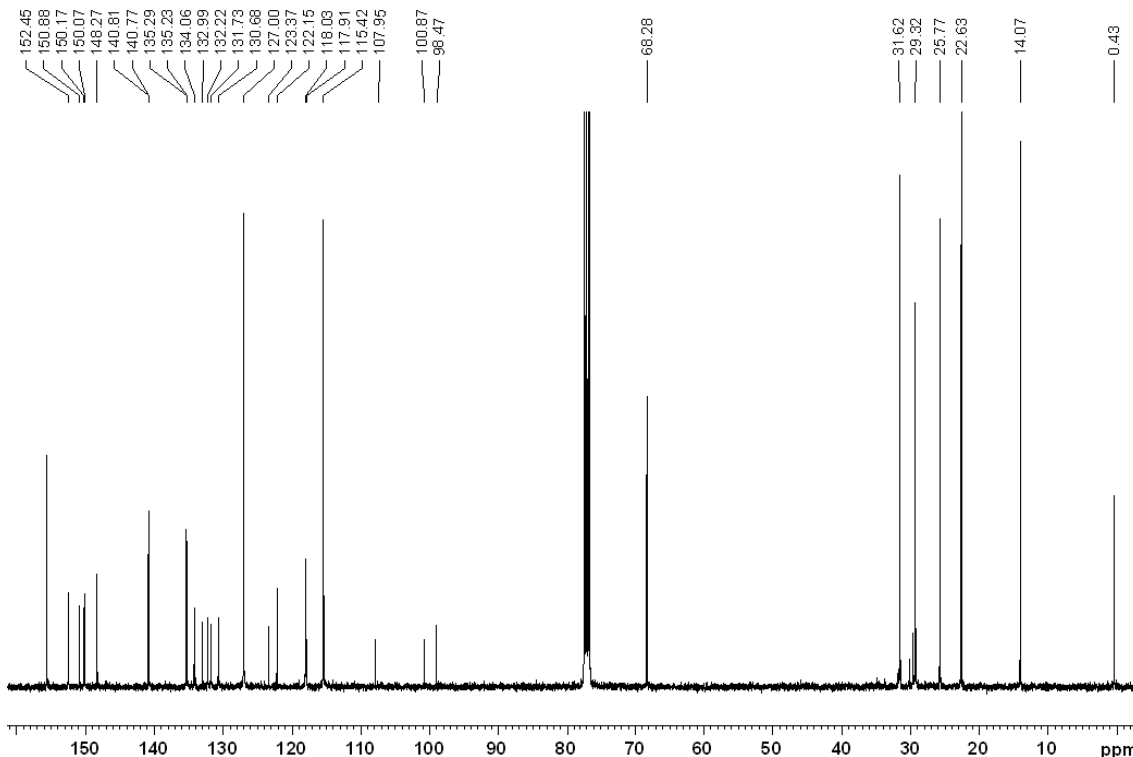


Figure S12. ¹³C NMR spectrum (100 MHz, CDCl₃) of compound 3b.

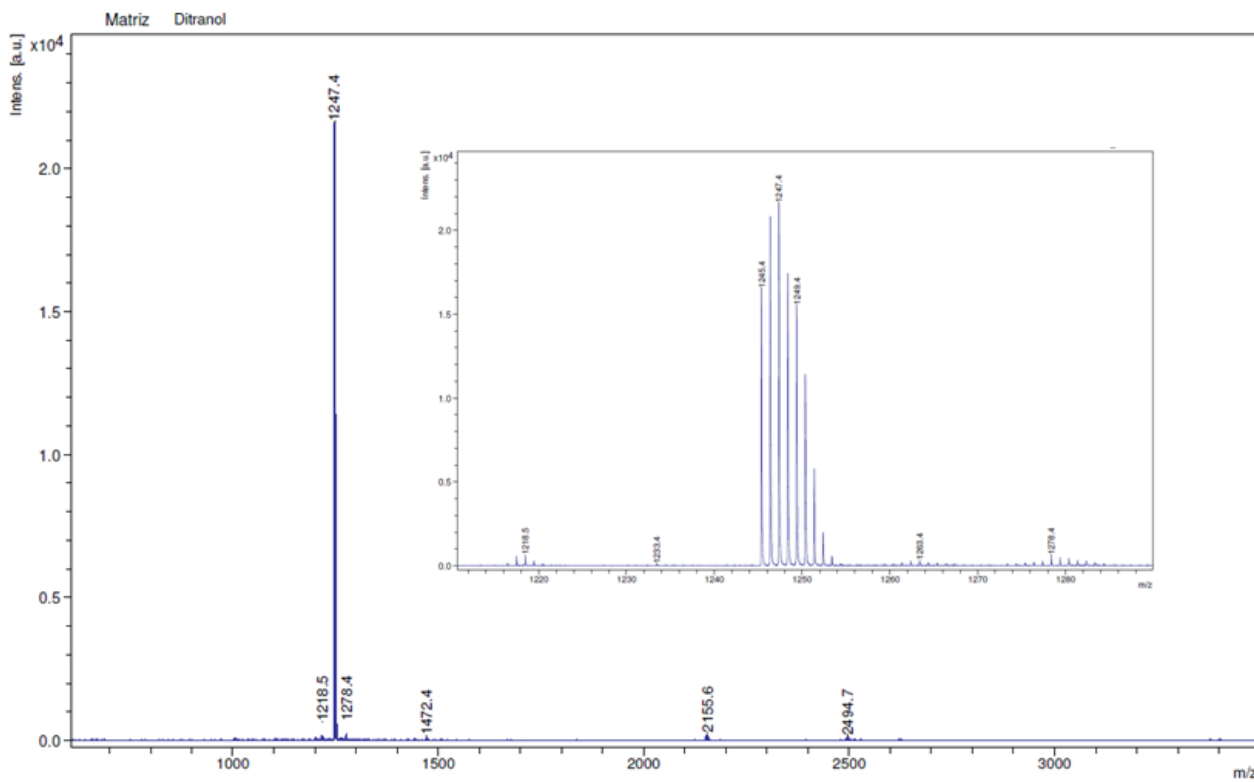


Figure S13. MALDI-MS spectrum of compound **1a** (Matrix: Ditranol).

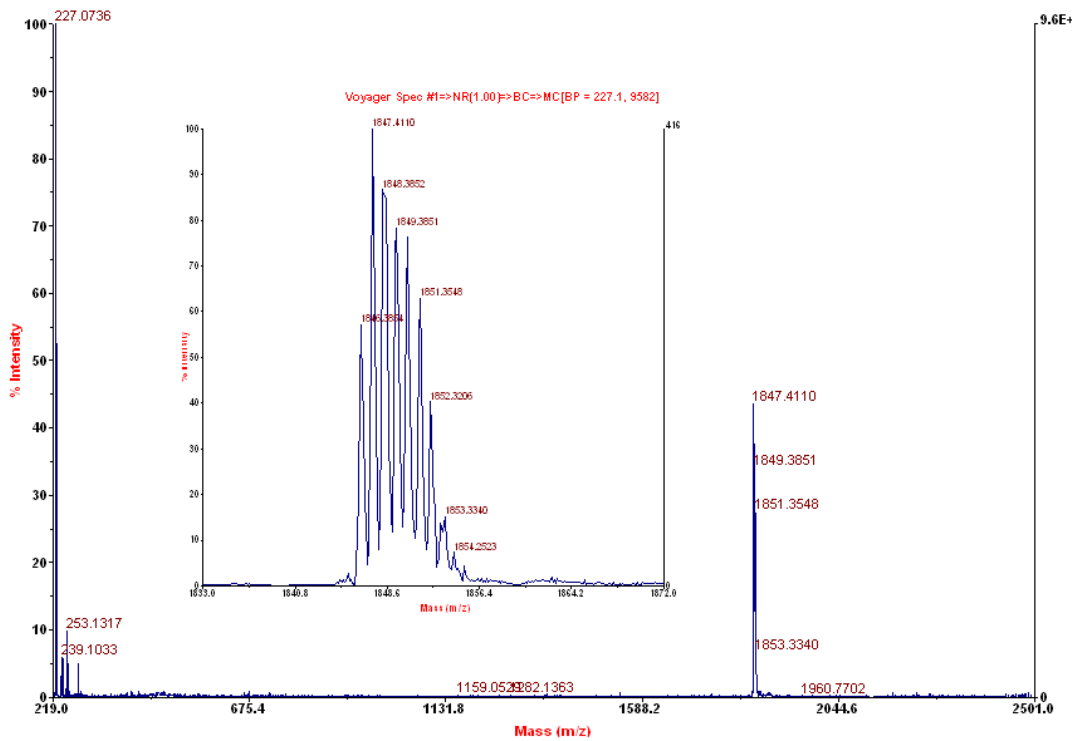


Figure S14. MALDI-MS spectrum of compound **1b** (Matrix: Ditranol).

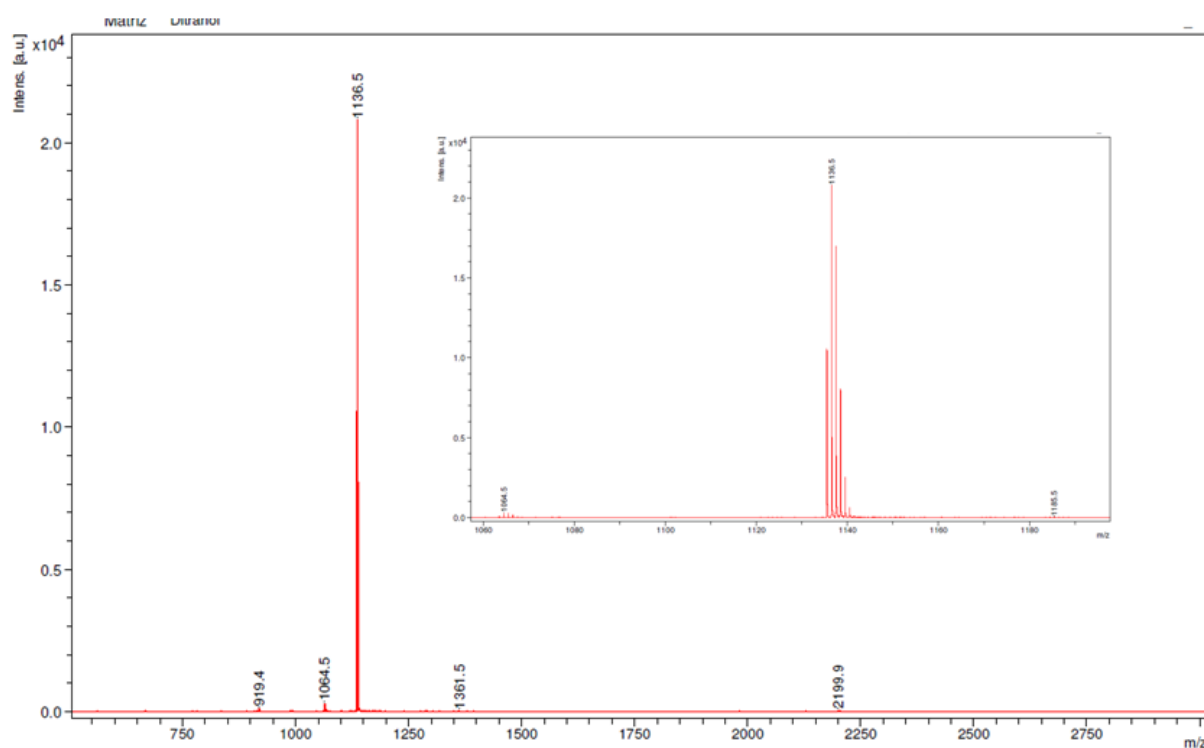


Figure S15. MALDI-MS spectrum of compound **2a** (Matrix: Ditranol).

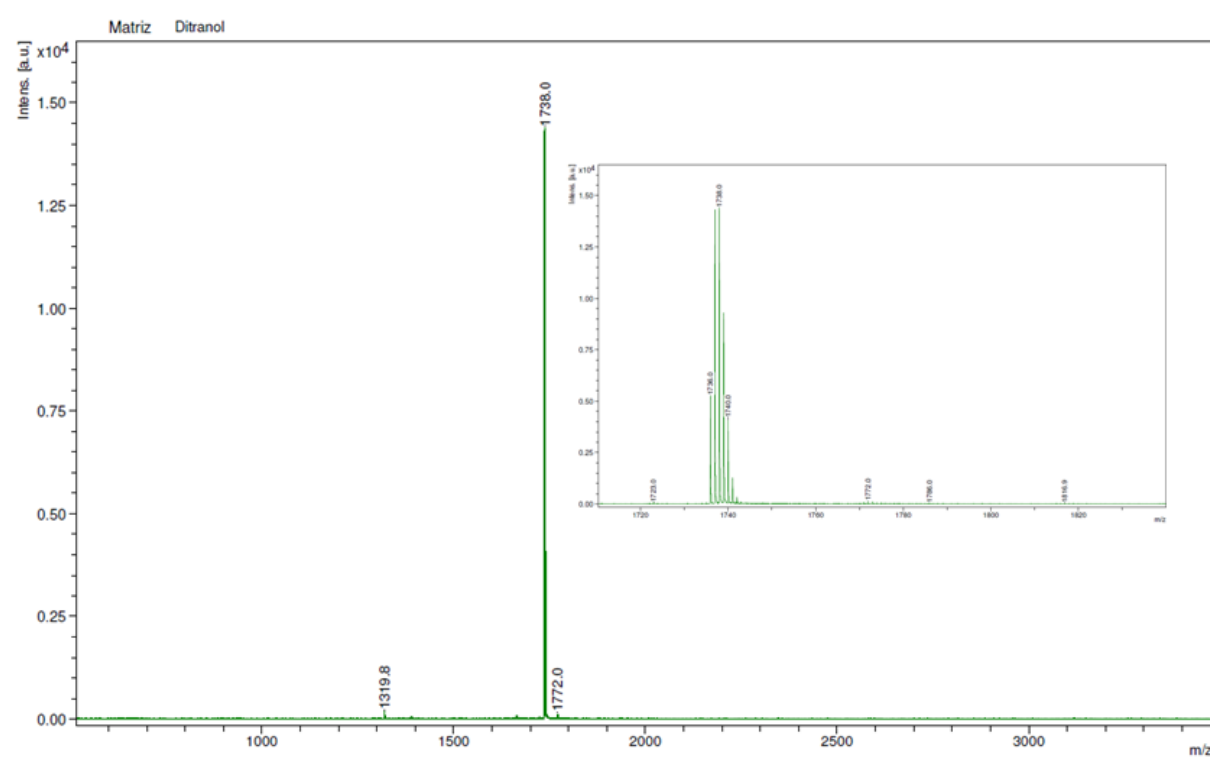


Figure S16. MALDI-MS spectrum of compound **2b** (Matrix: Ditranol).

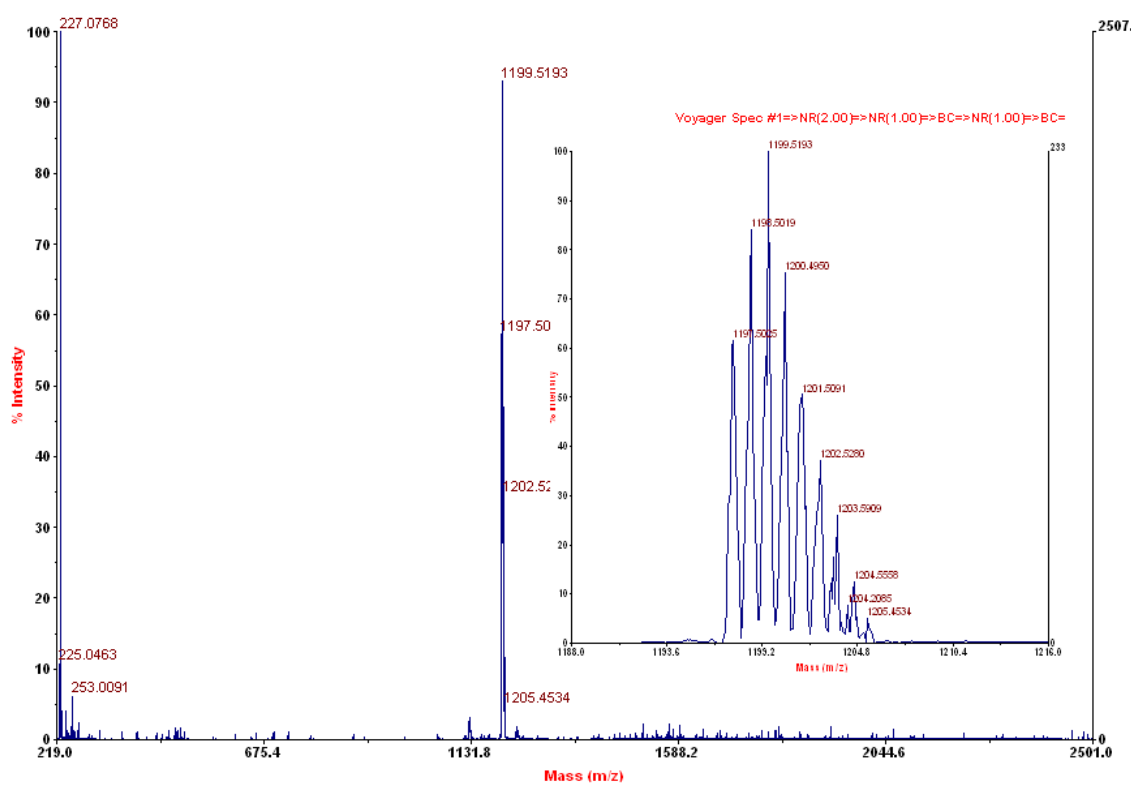


Figure S17. MALDI-MS spectrum of compound 3a (Matrix: Ditranol).

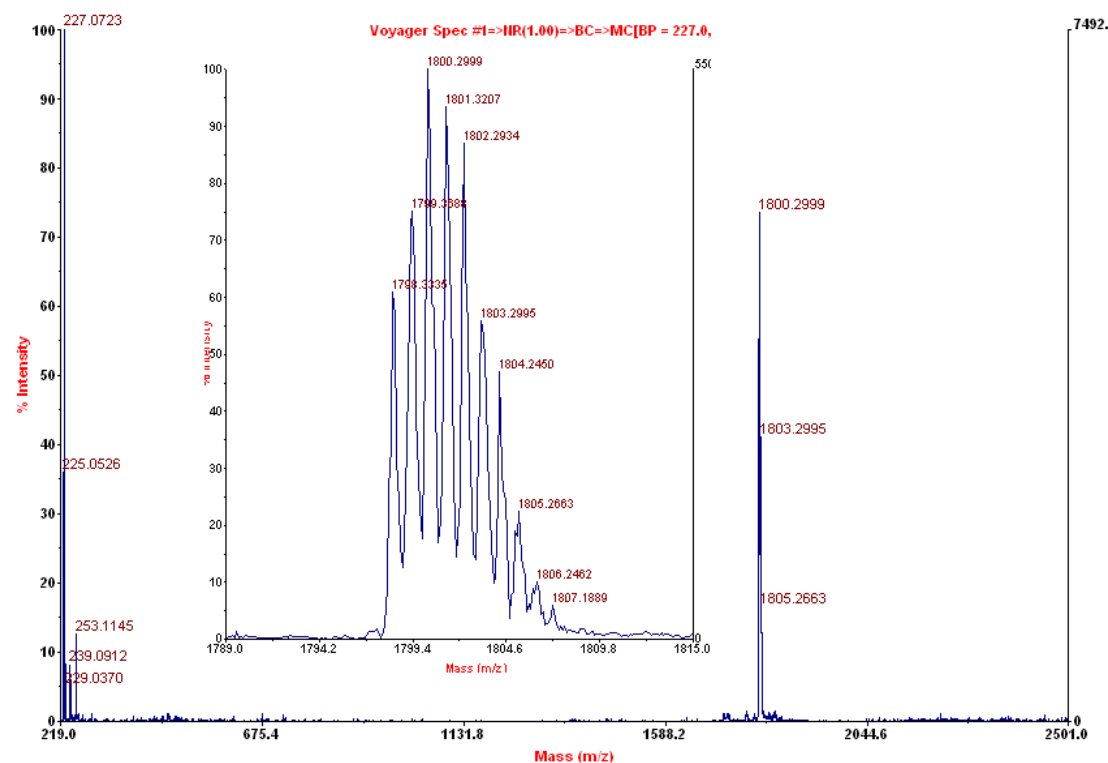


Figure S18. MALDI-MS spectrum of compound 3b (Matrix: Ditranol).

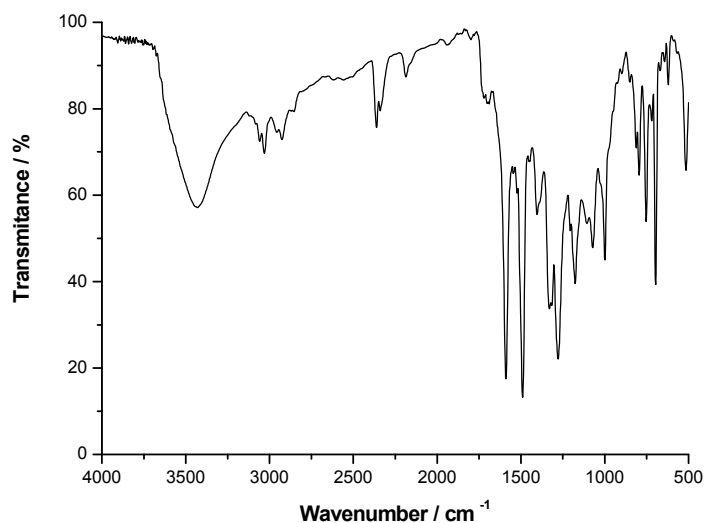


Figure S19. FT-IR spectrum of compound **1a** (KBr).

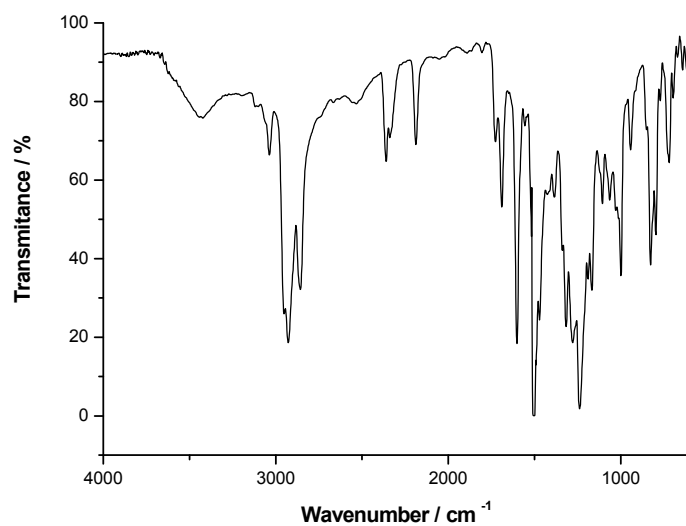


Figure S20. FT-IR spectrum of compound **1b**.

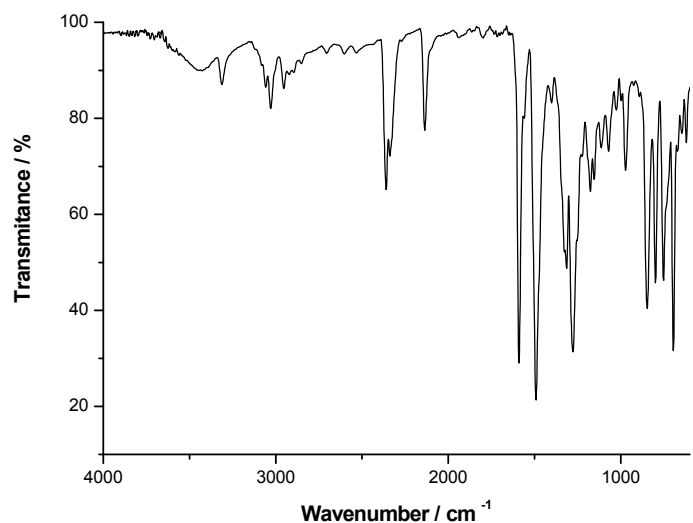


Figure S21. FT-IR spectrum of compound **2a**.

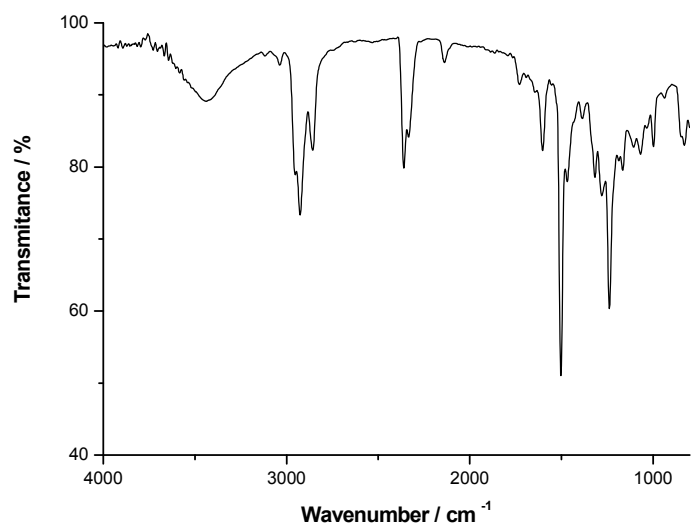


Figure S22. FT-IR spectrum of compound **2b**.

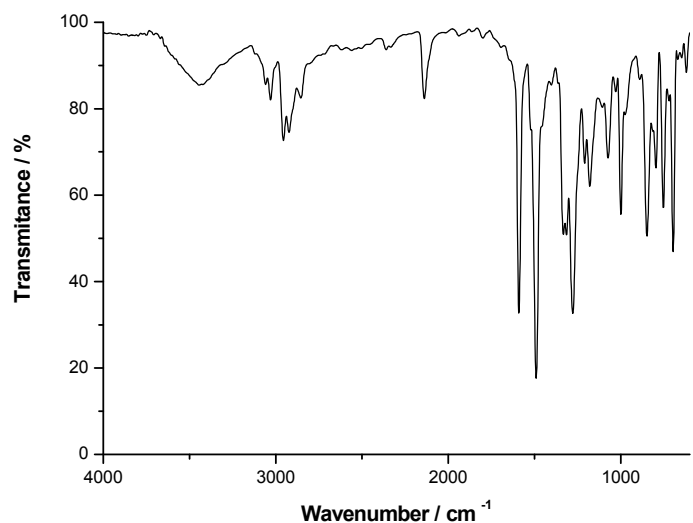


Figure S23. FT-IR spectrum of compound **3a**.

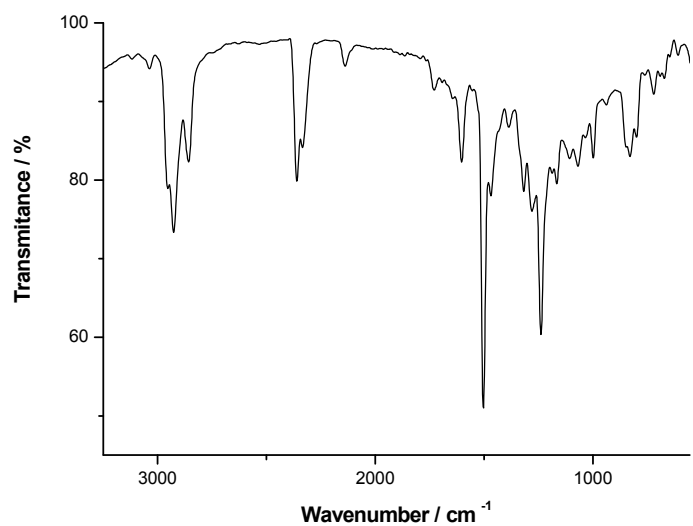
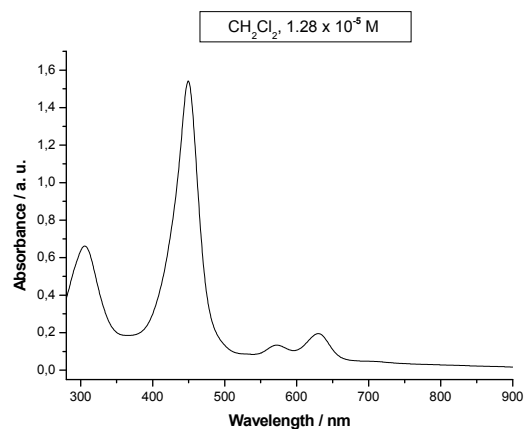


Figure S24. FT-IR spectrum of compound **3b**.

3.- UV-Visible and emission spectroscopies

A)



B)

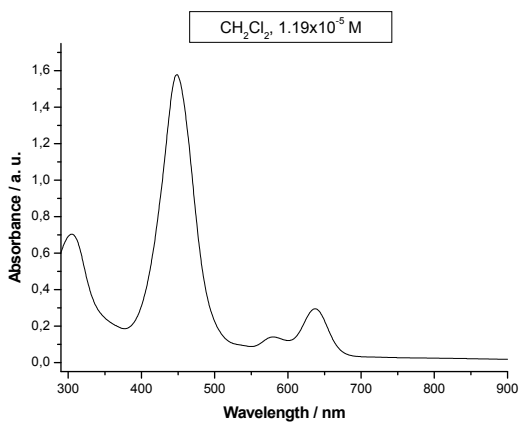
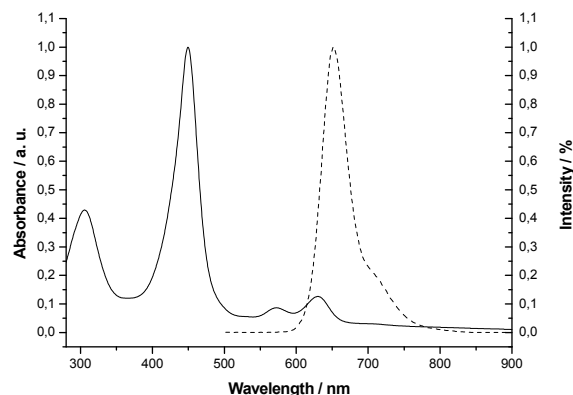


Figure S25. UV-Vis absorption spectra of compounds **1a** (A) and **1b** (B) in CH_2Cl_2 .

A)



B)

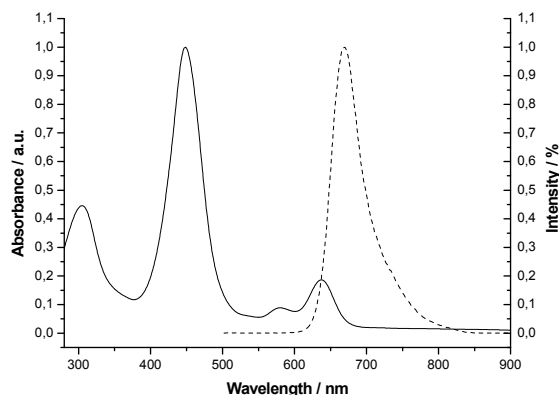
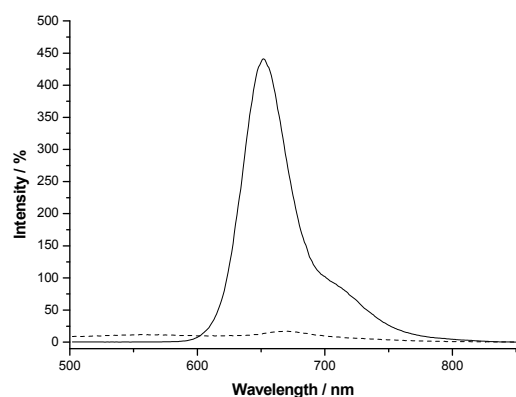


Figure S26. Normalized UV-Vis absorption and fluorescence emission spectra of compounds **1a** (A, $\lambda_{exc} = 450$ nm) and **1b** (B, $\lambda_{exc} = 449$ nm) in CH_2Cl_2 .

A)



B)

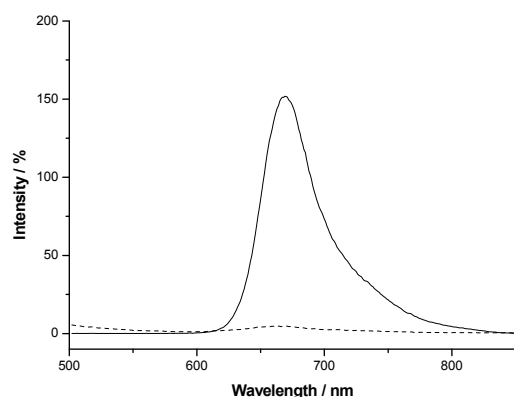


Figure S27. Fluorescence emission spectra in absence (solid line) and presence of TiO_2 (dash line) of **1b** in CH_2Cl_2 of compounds **1a** (A, $\lambda_{exc} = 450$ nm) and **1b** (B, $\lambda_{exc} = 449$ nm) in CH_2Cl_2 .

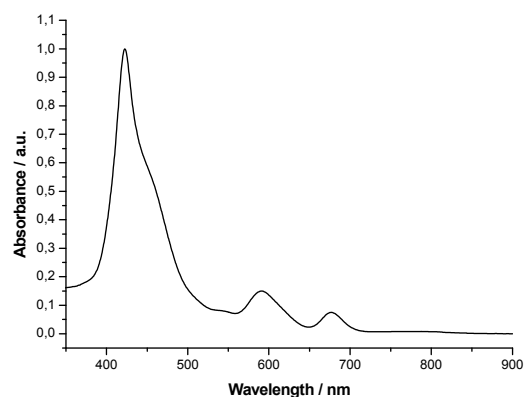
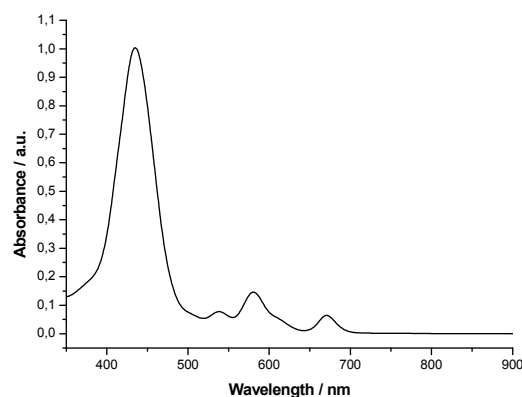


Figure S28. Normalized UV-Vis absorption spectra of compounds **2a** (A) and **2b** (B) in CH_2Cl_2 .

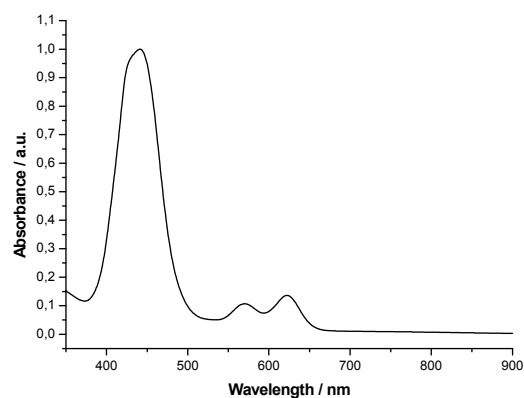
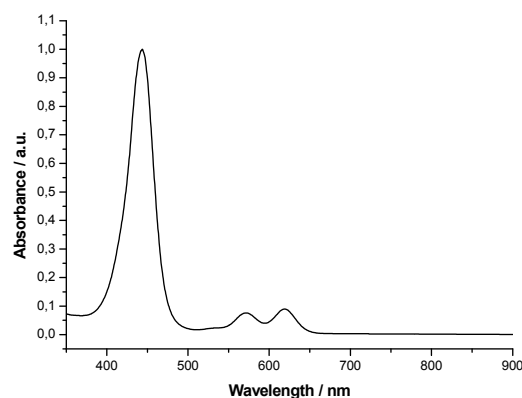


Figure S29. Normalized UV-Vis absorption spectra of compounds **3a** (A) and **3b** (B) in CH_2Cl_2 .

4-. Square Wave plots of 1a and 1b

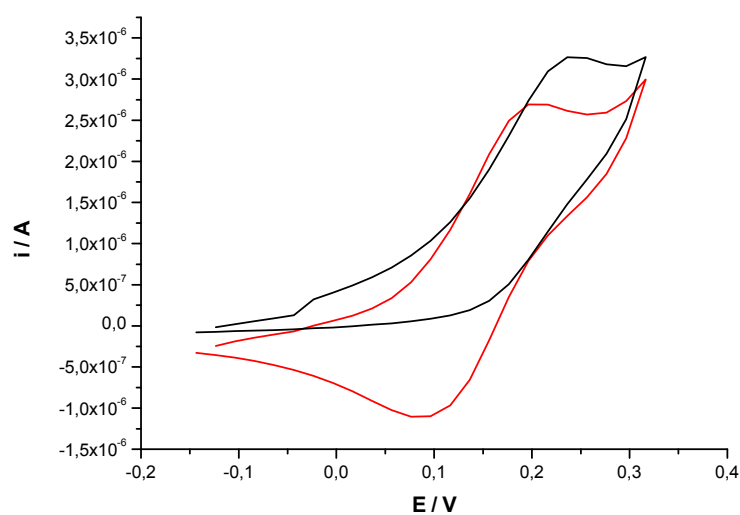


Figure S30. Cyclic Voltammetry (cathodic window) of compounds **1a** (black line) and **1b** (red line) (referred to Fc/Fc^+).

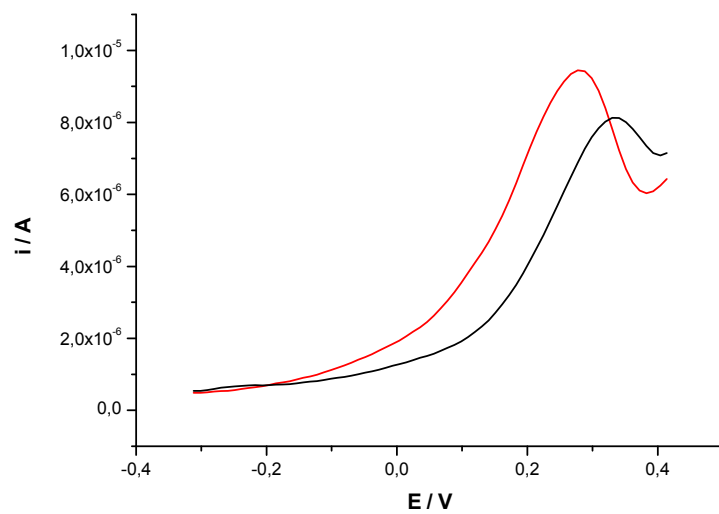


Figure S31. Square Ware Voltammetry plot (cathodic window) of compounds **1a** (black line) and **1b** (red line) (referred to Fc/Fc^+).

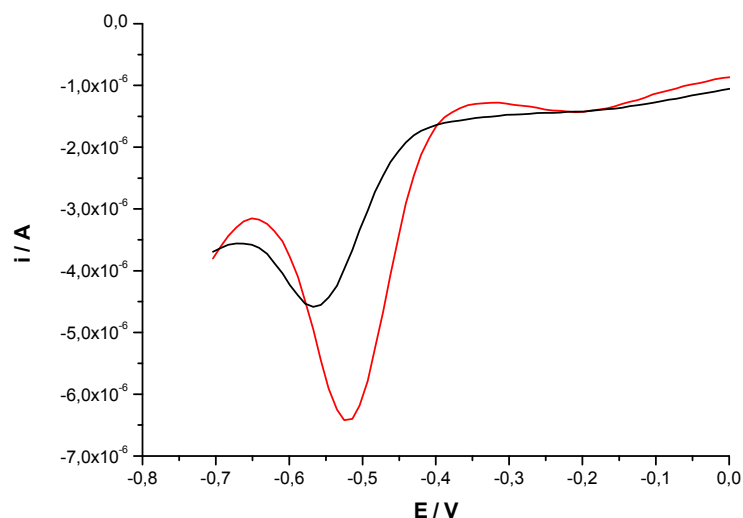


Figure S32. Square Ware Voltammetry plot (anodic window) of compounds **1a** (black line) and **1b** (red line) (referred to Fc/Fc⁺).

6.- Thermogravimetric analysis of 1a and 1b

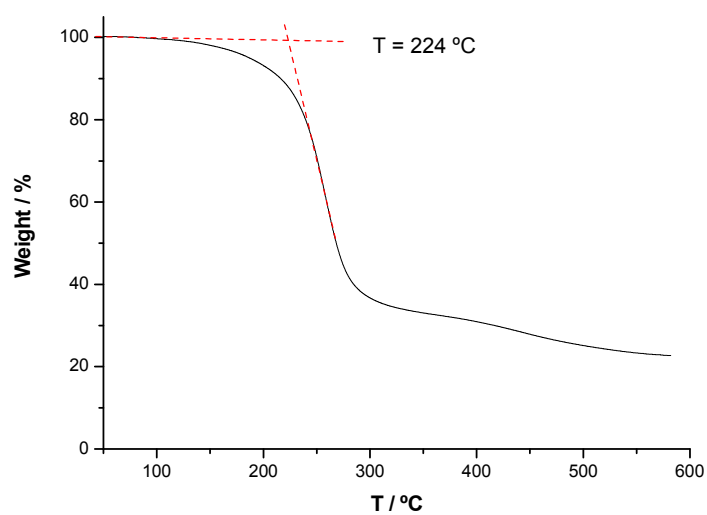


Figure S33. Thermogravimetric analysis of **1a**.

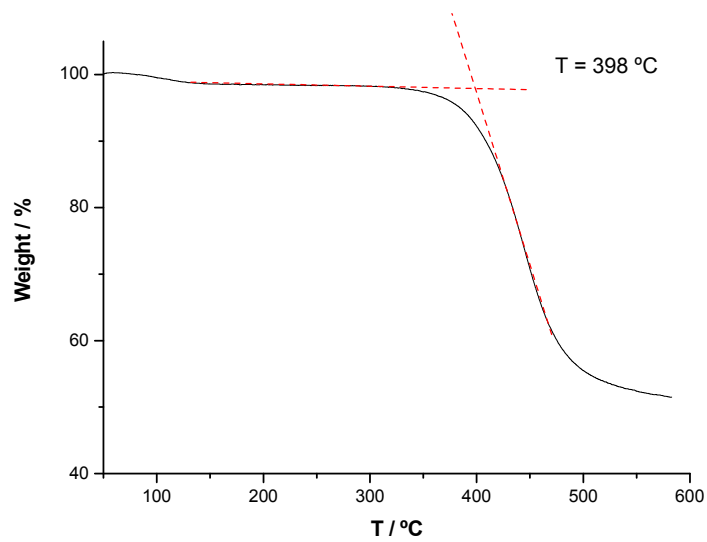


Figure S34. Thermogravimetric analysis of **1b**.